Photoemission study of chain- and layer-type TlS crystals

1997 J. Phys.: Condens. Matter 9 10271

(http://iopscience.iop.org/0953-8984/9/46/024)

J. Phys.: Condens. Matter **9** (1997) 10271–10282. Printed in the UK PII: S0953-8984(97)82733-6

Photoemission study of chain- and layer-type TlS crystals

S Kashida†, T Saito†, M Mori‡, Y Tezuka§ and S Shin§

† Faculty of Science, Niigata University, Ikarashi, Niigata 950-21, Japan

‡ School of Informatics and Sciences, Nagoya University, Furo-cho, Chikusa-ku, Nagoya 464-01, Japan

§ Institute for Solid State Physics, University of Tokyo, Tokyo 106, Japan

Received 15 March 1997, in final form 21 August 1997

Abstract. Thallium monosulphide is a mixed-valence compound containing monovalent and trivalent Tl ions. The compound crystallizes in two different structures, the tetragonal TlSe type and the monoclinic $TlGaSe_2$ type. Photoemission studies were carried out, using a synchrotron photon source, on TlS crystals with both the TlSe- and $TlGaSe_2$-type structures. Comparison of the spectra shows that the line shape of the Tl 5d core level is more asymmetric in the TlSe type than the $TlGaSe_2$ type. The asymmetry reflects the density of states near the Fermi level of the crystals. It was also found that as the incident photon energy increases the intensities of the valence band peaks increase relative to those of the Tl 5d core levels. Comparing the intensity ratios with the calculated photoionization cross section ratios, the characters of the valence bands were discussed.

1. Introduction

The ternary thallium chalcogenides $TlMX_2$ (M = Ga, In, X = S, Se, Te) crystallize in two different structures. The first is the tetragonal TlSe type [1]. This structure is characterized by linear chains formed of edge-connected MX_4 tetrahedra (see figure 1). Monovalent Tl ions are located between the chains and have eightfold coordination of the chalcogen ions. The second is the monoclinic $TlGaSe_2$ type [2]. The structure is characterized by layers formed of corner-connected MX_4 tetrahedra. These layers are stacked along the z-axis, where the successive layers are rotated with respect to each other by 90°. Monovalent thallium ions are located between the layers and have sixfold coordination of the chalcogen ions.

The ternary-layer-type thallium compounds, such as $TlGaSe_2$ and $TlInS_2$, are known to undergo successive phase transitions [3–5]. It is reported that their lowest-temperature phase is ferroelectric and the intermediate phase is incommensurate. Ferroelectric soft modes are observed in submillimetre dielectric measurements. The microscopic origin of the ferroelectricity is the stereochemical instability of the $6s^2$ lone-pair electrons [6]; that is, the distortion around a Tl^{1+} ion would cause Tl 6p orbitals to mix into the filled Tl 6s orbital and it stabilizes the ferroelectric structure by extending the band gap.

Thallium monosulphide belongs to this family. It is a mixed-valence compound containing monovalent and trivalent thallium ions as $Tl^{1+}(Tl^{3+}S_2^{2-})$. Recent x-ray studies have shown that TlS crystallizes both in the TlSe-type and the $TlGaSe_2$-type structures [7–9]. For brevity, we will hereafter call the former the chain type and the latter the layer type. Like the ternary thallium compounds, the layer-type TlS crystal undergoes successive ferroelectric phase transitions [9]. The microscopic origin of the phase transitions is the

0953-8984/97/4610271+12$19.50

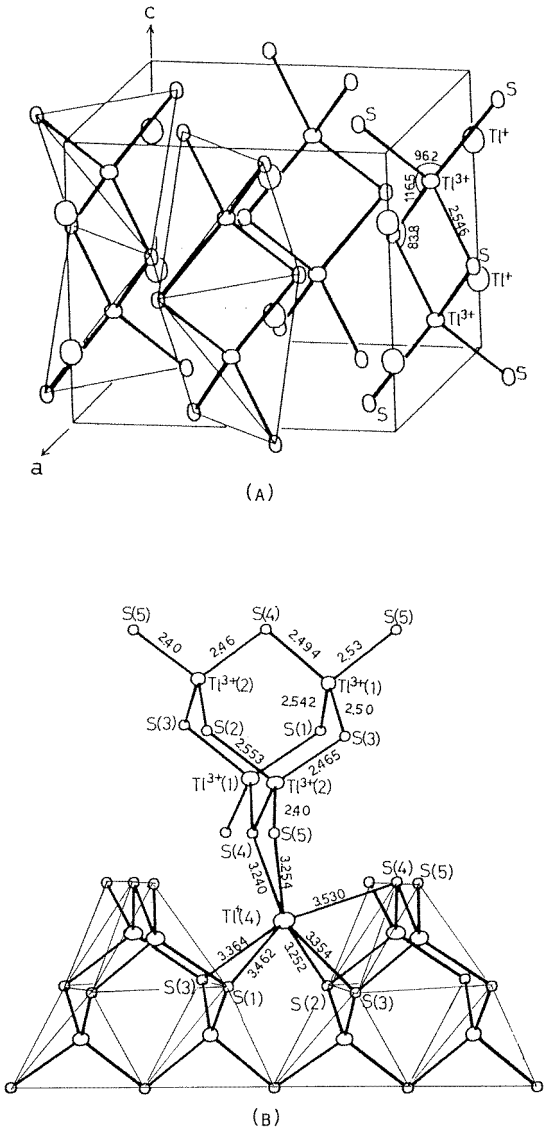

Figure 1. Schematic drawings of the two polymorphic structures in the thallium chalcogen compounds: (A) the tetragonal TlSe (chain) type, and (B) the monoclinic $TlGaSe_2$ (layer) type. For clarity, some of the tetrahedra are drawn with thin solid lines. (Taken from reference [13].)

small displacements of Tl^{1+} ions relative to apical S ions (cf. figure 1). Although TlS is known as a good photoconductor, its electronic structure is not well known. In order to study the valence band structure, ultraviolet photoemission spectra were taken. In an earlier x-ray photoemission study of the chain-type TlS, it was reported that no splitting of the 5d lines is observed for the two Tl ions having different valences [10]. In this study, using the synchrotron photon source, the energy dependences of the photoemission spectra were obtained for both the chain and layer types of TlS.

Figure 2. A photograph of TlS crystals; left: the tetragonal TlSe (chain) type; right: the monoclinic $TlGaSe_2$ (layer) type. Both types of crystal have shiny black colour, but a little different: brownish (chain type) and bluish (layer type).

2. Experimental details

Single crystal samples were grown from sulphur-rich melts. When the melts were cooled slowly we obtained needle-like crystals having the tetragonal TlSe-type structure, while when the melts were cooled rapidly we obtained platelet crystals which have the monoclinic $TlGaSe_2$-type structure (see figure 2). The electrical conductivities of the TlS crystals were measured by the two-terminal dc method. The conductivity of the layer-type TlS was about two orders of magnitude lower than that of the chain-type TlS (see figure 3). For comparison, measurements were also made for samples of Tl_2S and Tl metal.

The photoemission experiments were performed using synchrotron radiation from SOR-RING at the Institute for Solid State Physics, University of Tokyo. A combination of a modified Rowland-type monochromator and a double-pass cylindrical mirror analyser was used to measure the angle-integrated photoemission spectra [11]. The energy of the incident photons was 40 to 120 eV.

The samples were mounted with conducting epoxy cement on the sample holder. Clean surfaces were obtained by scraping the samples using a diamond file in a preparation chamber. The base pressure of this chamber was about 1×10^{-7} Pa. The samples were then transferred to the analyser chamber. The experiments were carried out at room temperature in a vacuum of 1×10^{-8} Pa. The surfaces of the samples were fairly stable; the experimental results did not change over the measured time of about 12–18 hours. In the case of the layer-type TlS, a charging effect was observed and an electron flood gun was used in order to suppress the charging of the sample.

The energy distribution curves (EDCs) were obtained by scanning the retardation voltage, where the analyser voltage was held constant. The relative transmission factor

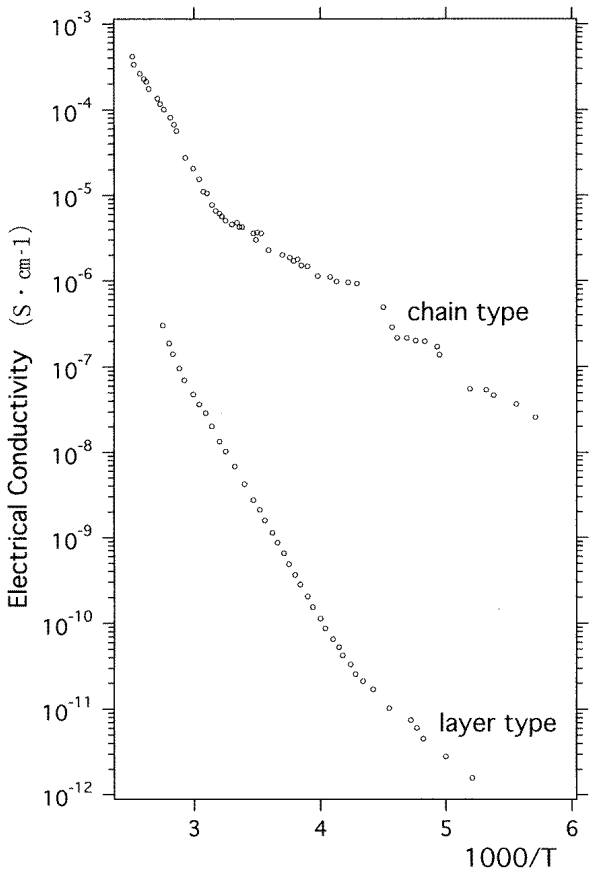

Figure 3. Temperature dependences of the electrical conductivities of the chain and layer types of TlS.

of the analyser was calibrated as a function of the retardation voltage. The overall energy resolution of the measurements was about 0.5 eV at an excitation energy of 80 eV. In the analysis of the EDCs, the contribution of the secondary electrons was corrected. Details of the calibration and correction procedures are described in [12].

Table 1. Binding energies of the Tl 5d core levels.

		Binding energy (eV)	
Sample	Tl valence	$5d_{5/2}$	$5d_{3/2}$
Tl metal	0	14.81	12.54
Tl_2S	1	15.55	13.36
TlS chain	1, 3	15.72	13.50
TlS layer	1, 3	15.81	13.59

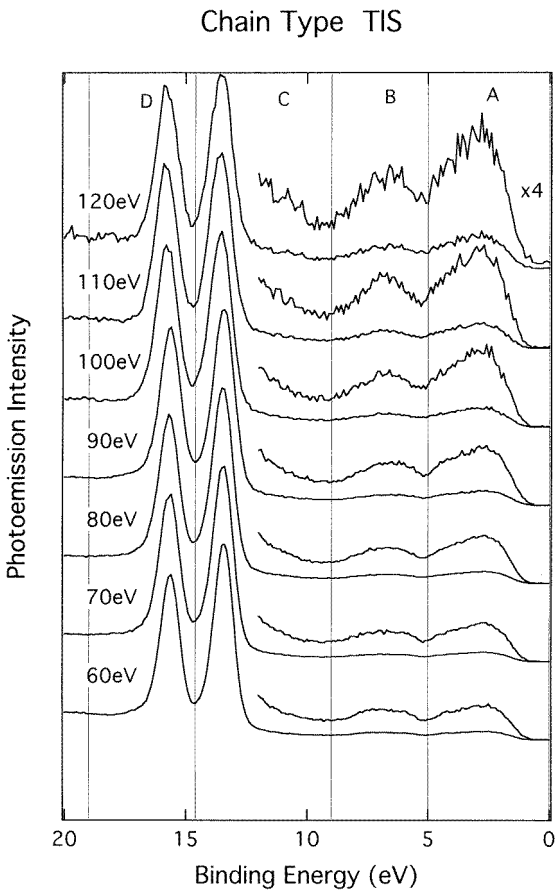

(a)

Figure 4. Photoelectron energy distribution curves (EDCs), taken with different incident photon energies. The spectra are normalized so that the Tl 5d levels have the same height. (a) Chain-type TlS, (b) layer-type TlS, and (c) Tl metal.

3. Results and discussion

Figure 4 shows the photoemission spectra of the chain and layer types of TlS and Tl metal, measured at different photon energies. The binding energies were determined from the Fermi edge of the Tl metal sample. The most prominent peaks in the measured energy range of 0–20 eV are those of Tl $5d_{3/2}$ and $5d_{5/2}$ core levels. In the chain and layer types of TlS, the positions of these 5d core levels agree within the experimental uncertainty. As the average valence of Tl atoms increases, the levels shift to higher binding energies (see table 1). The shift measures the charge transfer from the cations to the anions. However, for the two inequivalent cation sites in TlS, for Tl^{1+} and Tl^{3+}, the splitting of the 5d doublet is not observed, as already reported in reference [10]. A similar result was reported in an x-ray photoemission study of Pb_3O_4, which contains divalent and tetravalent Pb ions [13]. A qualitative interpretation can be made in terms of the shift of the Madelung energy at the Tl^{3+} site, since the anions are closer than is the case for the Tl^{1+} ions [13]. In order

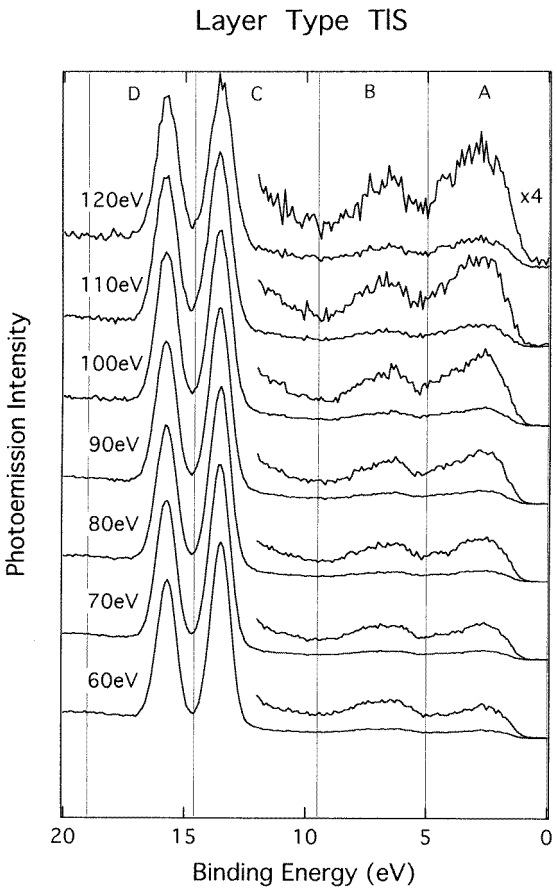

(b)

Figure 4. (Continued)

to clarify this point, however, detailed information on the electron correlation and bondings is necessary. A recent structural study of both types of TlS [14] showed that the distance Tl^{1+}–S (3.35 Å) is very close to the sum of the ionic radii of Tl^{1+} (1.47 Å) and S^{2-} (1.84 Å), while the distance Tl^{3+}–S (2.54 Å) is close to the sum of the covalent radii of Tl (1.58 Å) and S (1.07 Å).

A close inspection of the core Tl 5d spectra shows that the line shapes are asymmetric, i.e. the peaks have tails on the low-kinetic-energy (high-binding-energy) side. The asymmetry is caused by the many-electron effects which depend on the density of states at the Fermi level [15]. It is high for Tl metal but low for TlS. Hence, we observe asymmetric 5d lines for Tl metal but more symmetric lines for TlS samples. It will be noticed that the 5d levels of the chain-type TlS have more asymmetric line shapes than those of the layer-type TlS (see figure 5). This means that the chain-type TlS has a higher density of states near the Fermi level. This is consistent with the fact that the electrical conductivity of the chain-type TlS is higher than that of the layer-type TlS.

There is another process which gives rise to the line asymmetry: owing to the electron collisions, the escaping electron loses energy to the Fermi sea [15]. The probability of

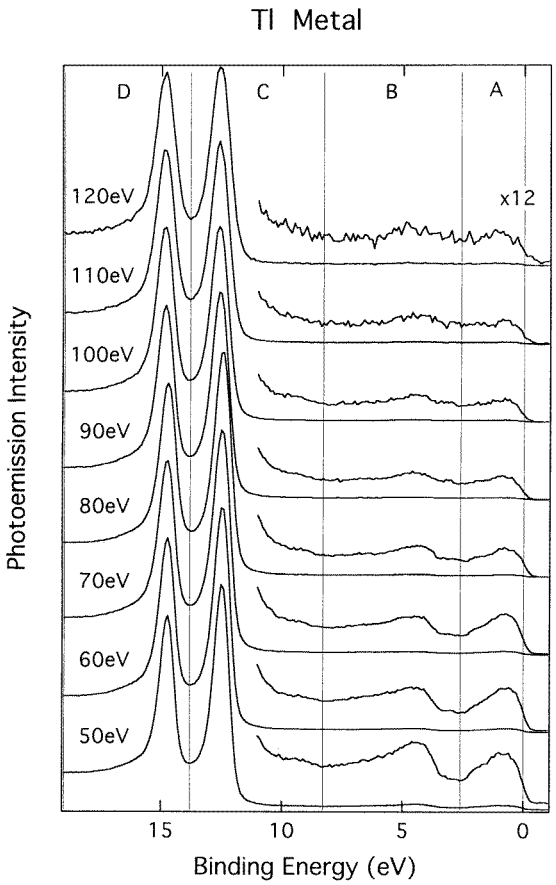

(c)

Figure 4. (Continued)

this process will decrease with increasing escape energy, while the above many-electron process is intrinsic and will not change with the kinetic energy of the electrons. These two processes may be distinguished by varying the incident photon energy. As the photon energy is increased, the asymmetry of the core levels shows no clear change in Tl metal, while in the case of the chain and layer types of TlS, the difference of the line shapes decreases (cf. figure 5), suggesting that the latter process is occurring at least in TlS.

Above the core 5d levels, broad valence band peaks are observed. The upper valence band edges are found around 0.95–1.05 eV below E_F. The edges are seen at almost the same positions in both the chain and layer types of TlS. For comparison, the intrinsic energy gaps are estimated, from the temperature dependence of the electrical conductivity (figure 3), as 0.94 eV and 0.90 eV for the chain and layer TlS, respectively. The photoemission intensity I_i is proportional to $\sigma_i \lambda$, where n_i is the density of electrons in the state i, σ_i is the photoionization cross section and λ is the escape depth. Here, we assume that the incident photon energy is sufficiently large that the effect of final-state densities can be ignored and that the energy variation of the escape depth can also be ignored. Figure 4 shows that as the photon energy increases in TlS the intensities of the valence band peaks increase relative

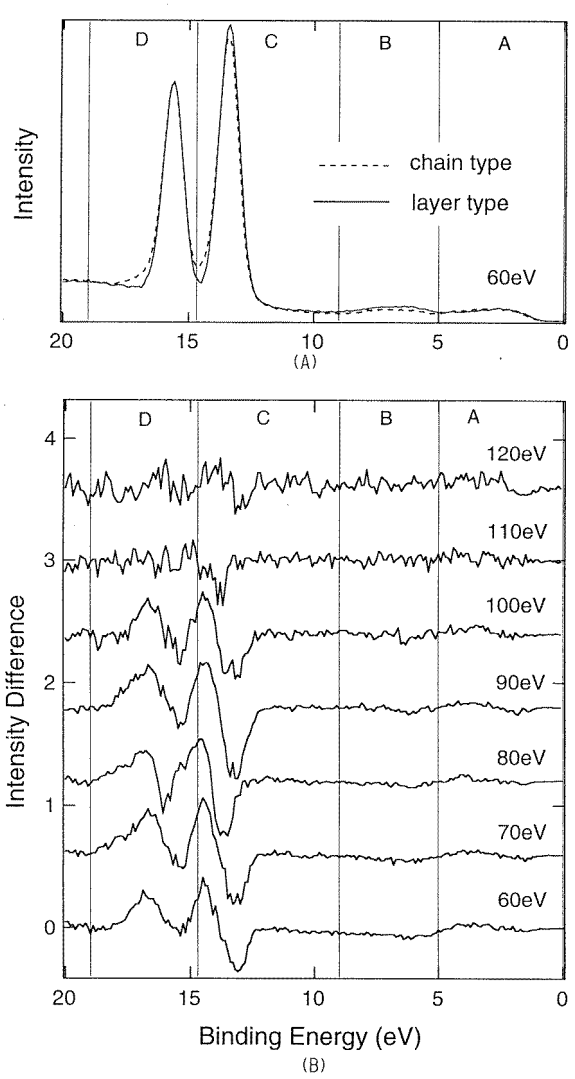

Figure 5. Comparison of the photoemission spectra of the chain and layer types of TlS (A), and the difference spectra (B). Note that in the chain-type TlS the Tl 5d levels have larger tails on the high-binding-energy side than the layer-type TlS, and that the difference decreases as the photon energy increases.

to those of the core Tl 5d levels, and that the situation is reversed in the Tl metal sample. The changes of the relative peak heights are attributed to the changes of the cross sections of Tl 5d, 6s and 6p levels and S 3s and 3p levels.

The valence band spectra may be divided into four areas: A (0–5 eV); B (5–9 eV); C: $5d_{5/2}$ (9–14.5 eV); and D: $5d_{3/2}$ (14.5–19 eV). The spectra of Tl metal are also divided: A (0–2.6 eV); B (2.6–8.3 eV); C: $5d_{5/2}$ (8.3–14 eV); and D: $5d_{3/2}$ (14–19 eV). The relative intensities are plotted in figure 6 as functions of the incident photon energy. For comparison, the calculated values of the photoionization cross sections are taken from [16] and plotted in figure 7. The cross sections of Tl 6s, and S 3s and 3p states, normalized to that of the Tl

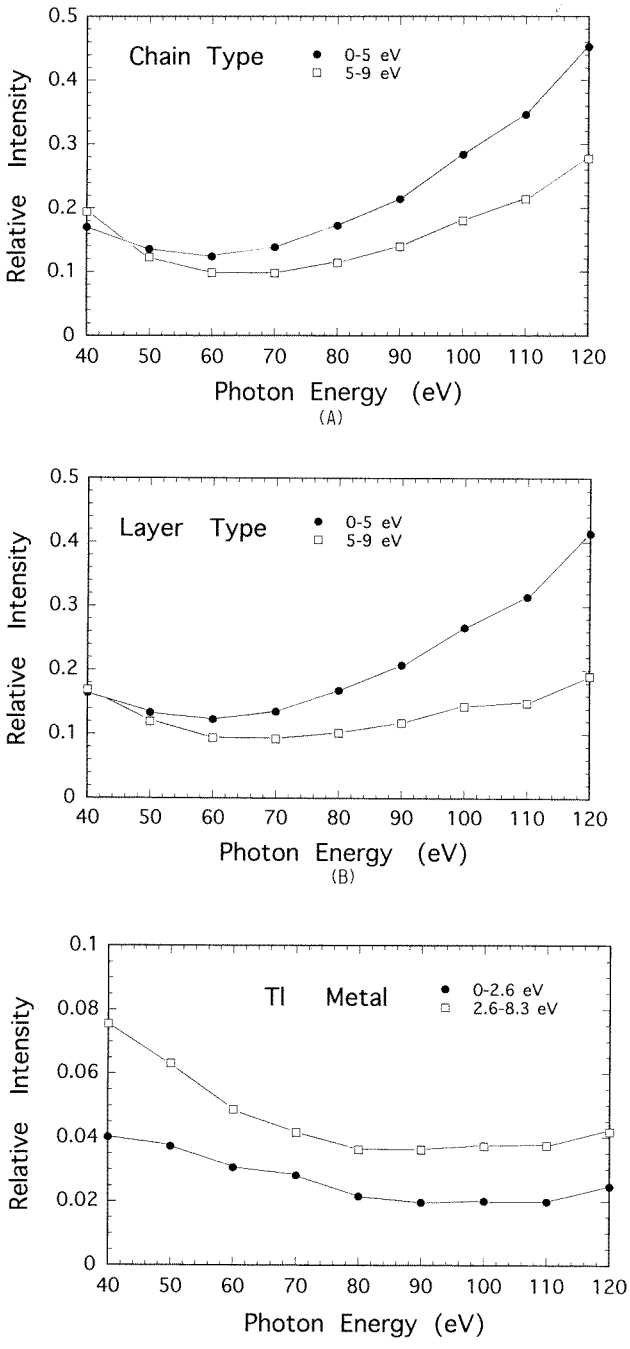

Figure 6. Relative intensities of the peaks A and B, normalized to the intensity of the core peak C ($5d_{5/2}$) and plotted against the photon energy.

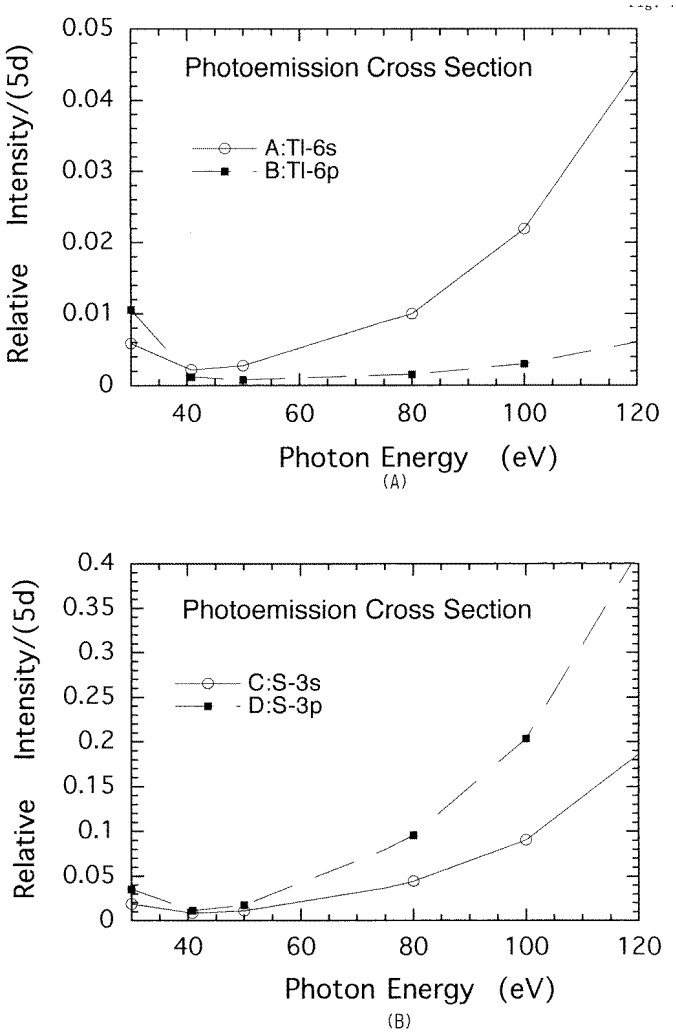

Figure 7. Calculated photoemission cross sections of (A) Tl 6s and 6p and (B) S 3s and 3p orbitals, normalized to that of the Tl 5d orbital and plotted against the incident photon energy. (Data taken from reference [16].)

$5d_{5/2}$ state, increase as the photon energy increases, but for the Tl 6p state the curve shows a different behaviour. By comparing the observed values with the calculated cross section ratios, we can identify the valence band structure.

First, we briefly discuss the spectra of Tl metal. The valence band of Tl metal contains only Tl 6s and 6p states, and will be simpler than those of the TlS compounds. The valence band spectra of Tl metal show a photon energy dependence similar to that of the Tl 6p state; as is seen in figure 6(C), the relative peak height decreases as the photon energy increases. There is, however, definite deviation; the calculated cross section σ of the Tl 5d level has a peak at around 42 eV (nearly twice the binding energy of the Tl 5d level), while the intensity ratio curves show minima at about 70 eV. In the solid state the wave functions will change from those of the atomic state; therefore, the choice of the correct σ-values in

the analysis is problematic. The electron correlation effect will become important close to the threshold where the escaping electrons travel slowly and have a lot of time to interact with the rest of the electrons in the solid [17]. The energy dependence of the escape depth λ and the density of the final states may not be ignored. Nevertheless, it should be noticed that there is no essential difference between the features of the bands A and B. It is in contrast to the previous conjecture [18] that the upper band is formed mainly of Tl 6p states while the lower band is formed of Tl 6s states. The experimental spectra may suggest that the contribution of the Tl 6s electron is not significant.

As far as the authors are aware, the band structure of TlS has not been reported. The only exception is a work on the Tl^{1+} chains of tetragonal TlS studied within the extended Hückel framework [19]. Therefore, only a qualitative analysis is made here. Comparing the calculated and observed values shown in figures 6 and 7, we can say that band A of TlS is formed mainly of S 3p states, and that the S 3s orbital is far below and around the Tl 5d core level. The cross section of the Tl 6s state is about one order of magnitude lower than that of the S 3p state. The relative intensity of the inner band B rises on the low-incident-photon-energy side. This fact suggests that, as in the case of Tl metal, band B is derived from the Tl 6p states as well as the S 3p and Tl 6s states.

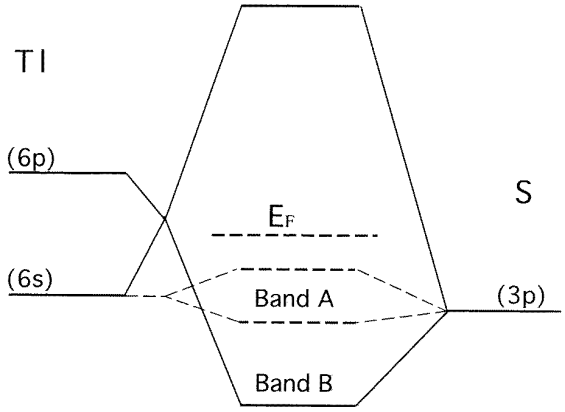

Figure 8. A schematic drawing of the energy levels in TlS. Around a Tl^{3+} ion, Tl 6s, 6p and S 3p electrons form strong sp^3-type bonding and antibonding states, while around a Tl^{1+} ion lone-pair electrons of Tl 6s and S 3p form weak bonding and antibonding states both of which are occupied (see the text).

The bonding within the $Tl^{3+}S_4$ tetrahedra is considered as covalent and of the sp^3 type. The bonding orbitals are centred on the more electronegative S atoms. A schematic representation of the energy diagram is given in figure 8. The diagram suggests that the hybrid bonding orbitals make the inner band peak B. We can see from figure 6 that the band B of the layer-type TlS shows larger contributions from Tl 6p states than the chain-type TlS; thus, the spectra show a variation with the polymorphs. The different features of the peak B in the chain- and layer-type TlS are related to the differences in the structures [14]: the edge-connected or the corner-connected $Tl^{3+}S_4$ tetrahedra; the $Tl^{3+}S$ distances (2.54 Å and 2.50 Å); and the elongation of the tetrahedra in the chain type (cf. figure 1)).

The non-bonding S 3p (lone-pair) electrons are at the top of the valence band and form the peak A. This peak also contains weak hybrid orbitals of Tl^{1+} ions and the surrounding S ions; these are mainly of S 3p and Tl 6s (lone-pair) orbitals; both the bonding and the

antibonding orbitals are occupied. The top of this band, along with the lowest conduction band (mainly composed of Tl 6p states), takes a decisive part in the determination of the semiconducting and dielectric properties of the compounds. The Tl^{1+}–Tl^{1+} distance is 3.40 Å in the chain-type TlS, it is comparable with 3.35 Å in Tl metal, and it is somewhat shorter than 3.93 Å in the layer-type TlS [14]. Considering that TlS crystals are p-type semiconductors and the above asymmetry of the Tl 5d lines, we may conclude that in the chain-type TlS the states near the Fermi level are derived from the Tl 6s state in the Tl^{1+} contact chains. The role of the Tl 6s orbitals will be our primary concern. However, from the energy dependence of the intensity alone, we cannot distinguish Tl 6s state from S 3p states, since for these two orbitals the cross sections have similar energy dependences.

In this study, photoemission studies were performed, and the electronic structures of the two TlS polymorphs were discussed from two viewpoints: first, on the basis of the asymmetry in the 5d core line shapes, and second, on the basis of the energy dependence of the valence band peaks. In order to identify the role of Tl 6s lone-pair state, further experimental end theoretical studies are necessary. Photoelectron spectroscopy at lower incident photon energies may be helpful, and detailed band-structure calculations are also necessary.

Acknowledgments

The authors are indebted to T Matsukawa, Naruto University of Education, for help. They also thank the staff of SOR-RING, Institute for Solid State Physics, University of Tokyo, for excellent support. This study was supported by the Cooperative Research Programme (1995) of the Institute for Solid State Physics, University of Tokyo, and by a Grant-in-Aid for Scientific Research in a Priority Area from the Ministry of Education, Science and Culture. The preliminary experiments were done using an XPS spectrometer at the Centre for Cooperative Research, Niigata University.

References

[1] Ketelaar J A A, t'Hart W H, Moerel M and Polder D 1939 *Z. Kristallogr.* **101** 396
[2] Muller D and Hahn H 1978 *Z. Anorg. Allg. Chem.* **438** 258
[3] Allakhverdiev K, Sardarly R, Wondre F and Ryan J F 1978 *Phys. Status Solidi* b **88** K5
[4] Volkov A A, Goncharov Yu A, Kozlov G V, Allakhverdiev K R and Sardarly R M 1983 *Sov. Phys.–Solid State* **25** 2061
[5] Hochheimer H G, Gmelin E, Bauhofer W, von Schnering-Schwartz C, von Schnering H G, Ihringer J and Appel W 1988 *Z. Phys.* B **73** 257
[6] Orgel L E 1959 *J. Chem. Soc.* **4** 3815
[7] Kashida S, Nakamura K and Katayama S 1992 *Solid State Commun.* **82** 127
[8] Kashida S, Nakamura K and Katayama S 1993 *J. Phys.: Condens. Matter* **5** 4243
[9] Nakamura K and Kashida S 1993 *J. Phys. Soc. Japan* **62** 3135
[10] Porte L and Tranquard A 1980 *J. Solid State Chem.* **35** 59
[11] Kakizaki A, Sugawara H, Nagakura I and Ishii T 1980 *J. Phys. Soc. Japan* **49** 2183
[12] Soda K, Mori T, Taniguchi M, Asaoka S, Naito K, Onuki Y, Komatsubara T, Miyahara T, Sato S and Ishii T 1986 *J. Phys. Soc. Japan* **55** 1709
[13] Thomas J M and Michael J T 1974 *J. Chem. Soc. Faraday Trans.* II **70** 329
[14] Kashida S and Nakamura K 1994 *J. Solid State Chem.* **110** 264
[15] Doniach S and Sunjic M 1970 *J. Phys. C: Solid State Phys.* **3** 285
[16] Yeh J J and Lindau I 1985 *At. Data Nucl. Data Tables* **32** 1
[17] Johansson L I, Lindau I, Hecht M, Goldberg S M and Fadley C S 1979 *Phys. Rev.* B **20** 4126
[18] Ley L, Pollak R, Kowalczyk S and Shirley D A 1972 *Phys. Lett.* **23** 429
[19] Janiak C and Hoffmann R 1990 *J. Am. Chem. Soc.* **112** 5924